Northumbria Research Link

BPSK Subcarrier Intensity Modulated Free-Space Optical Communications in Atmospheric Turbulence

Wasiu O. Popoola, *Student Member, IEEE*, and Zabih Ghassemlooy, *Senior Member, IEEE*

Abstract—**Free-space optical communications (FSO) propagated over a clear atmosphere suffers from irradiance fluctuation caused by small but random atmospheric temperature fluctuations. This results in decreased signal-to-noise ratio (SNR) and consequently impaired performance. In this paper, the error performance of the FSO using a subcarrier intensity modulation (SIM) based on a binary phase shift keying (BPSK) scheme in a clear but turbulent atmosphere is presented. To evaluate the system error performance in turbulence regimes from weak to strong, the probability density function (pdf) of the received irradiance after traversing the atmosphere is modelled using the gamma-gamma distribution while the negative exponential distribution is used to model turbulence in the saturation region and beyond. The effect of turbulence induced irradiance fluctuation is mitigated using spatial diversity at the receiver. With reference to the single photodetector case, up to 12 dB gain in the electrical SNR is predicted with two direct detection PIN photodetectors in strong atmospheric turbulence.**

Index Terms—**Atmospheric turbulence, diversity, free-space optics (FSO), gamma-gamma distribution, negative exponential distribution, subcarrier modulation.**

I. INTRODUCTION

FREE-SPACE optical communications (FSO) is a promising technology capable of offering full-duplex gigabit rate throughput (data, voice, and video simultaneously) in certain applications and environment [1]–[3]. FSO offers a huge license-free frequency spectrum using a single wavelength, immunity to electromagnetic interference including co/adjacent channel interference (due to a well defined narrow beam size and no power spill), and high security [1], [4]. The technology is fundamentally based on transmitting data laden light through the atmosphere and collecting the light by a telescope at a remote distance. It offers data rates comparable to optical fiber communications but at a fraction of its deployment cost. Further more, its extremely narrow laser beam width offers spatial multiplexing and multiple links capabilities in a given location. The transmitted optical beam traversing the atmosphere can be absorbed, scattered or displaced depending on the atmospheric condition, thus setting the fundamental limits of FSO systems. Compared with the RF system, FSO is

less affected by snow and rain, but can be severely affected by the atmospheric turbulence and fog.

Generally, FSO wavelength is chosen to coincide with the low atmospheric absorption windows making the Mie scattering induced by the fog, haze and the aerosol to be the dominant source of irradiance attenuation. The value of the attenuation coefficient cannot be calculated *a priori* because of the complex shapes and orientations of the particles. Experimental values obtained have suggested that dense fog can result in extinction coefficient of up to 270 dB/km [1]. Interestingly, the irradiance attenuation due to thick fog, snow and haze is found to be wavelength independent [3]. Therefore, FSO systems leverage on existing optical sources and photodetectors used in optical fiber communication. During dense fog, to meet the high availability requirements of the telecoms industry (over 99.9% availability), the FSO range is only limited to around 500 m [2], [3] where sufficient link margin is available. For longer distances in such condition, an FSO link backed up by a complementary RF link at lower data rate would be the preferred option.

However, in clear atmosphere, with a typical attenuation coefficient of 0.43 dB/km, a longer range FSO (>1 km) is easily achievable. A major challenge facing FSO systems in clear atmosphere is the effect of turbulence induced irradiance fluctuation on the system performance especially for a link range exceeding 1 km [5]–[8]. The irradiance fluctuation (scintillation) is caused by small temperature fluctuations (0.01 to 0.1 degree) on the spatial scale of 0.1 cm to 10 m, which causes changes in the refractive index of the atmosphere [2]. To fully study, understand and predict FSO performance under a clear atmospheric condition, the knowledge of statistical distribution of atmospheric turbulence is essential. Although, turbulence is very well studied and a number of models have been developed to describe it; however, most models do not address turbulence across all regimes [9]. One widely reported model is the log normal turbulence model which is only valid for a weak regime as reported in [6], [9], [10]. Irradiance fluctuation (scintillation) caused by the atmospheric turbulence could result in deep signal fades that lasts for $\sim 1-100$ μs [11], [12]. For a link operating at say 1 Gbps, this could result in the loss of up to 10^5 consecutive bits. To avoid this huge data loss, turbulence induced irradiance fluctuation must therefore be mitigated. In [13] error control coding has been proposed, however the huge amount of redundant bits required in deep fades could result in prohibitive processing delay and efficiency degradation.

Although an on-off keying (OOK) intensity modulated based FSO link is widely reported, its major challenge lies in the fact that it requires adaptive threshold to perform optimally in atmospheric turbulence condition [8], [10], [14]. To circumvent this implementation difficulty and to ameliorate turbulence induced irradiance fluctuation, we consider in this paper the SIM

that is based on the BPSK scheme together with an array of N-PIN photodetectors. Moreover, in the present communication networks especially in CATV over fiber links, subcarriers are used [15], [16] and for the seamless integration of FSO into the present and in fact the future communication networks, the study of subcarrier modulated FSO is indeed worthwhile. The atmospheric turbulence across weak to strong regime is modelled using the gamma-gamma distribution [13], [17], [18] while negative exponential turbulence model is used in the limit of strong turbulence. And the noise, which is modelled as additive white Gaussian comprises of both the background radiation and the thermal noise. The remainder of the paper is arranged as follows: Section II discusses atmospheric turbulence; subcarrier intensity modulation is discussed in Section III while Sections IV and V give the bit-error rate (BER) performance metric and the conclusion, respectively.

II. ATMOSPHERIC TURBULENCE

When a laser radiation propagates through the atmosphere, it does experience amplitude and phase fluctuations due to atmospheric turbulence. This effect is the consequence of random variations in the atmospheric index of refraction due to corresponding changes in atmospheric temperature. According to [9], the induced thermal gradients may be viewed as close-packed spherical regions or eddies having statistically varying diameters and indexes of refraction. The Taylor's frozen-flow often applied to atmospheric turbulence [9], [19] suggests that turbulent eddies are fixed in the atmosphere and only move with the wind. The theory goes on to suggest that the temporal variations in the atmospheric index of refraction are primarily due the component of the local wind velocity perpendicular to the beam propagation direction. The temporal coherence time τ_0 of atmospheric turbulence is known to be in the order of millisecond, which is very large compared to a typical data symbol duration T. Hence, the channel is frozen over the duration of more than one symbol.

Atmospheric turbulence is well studied and various models exist to describe it. The mostly reported model is apparently the log normal turbulence [14], [20], [21]. This model has gained considerable attention in the literature because it is mathematically convenient and tractable. The log normal model is based on the Rytov approximation, which requires the magnitude of the scattered field wave to be small compared to the unperturbed phase gradient [19]. Unfortunately, this assumption is only valid in single scattering event characterizing weak turbulence. When multiple scatterings are experienced especially in longer link ranges, the incident wave becomes increasingly incoherent and log normal model becomes invalid [9], [18], [19].

An important parameter that describes the strength of turbulence is the log intensity variance σ_l^2. The scintillation index defined by $S.I. = (E[I^2]/(E[I])^2) - 1$ is another valid parameter for describing the turbulence strength, where $E[.]$ represents the expectation. In fact, $S.I.$ is the log intensity variance normalized by the square of the mean irradiance. It is sometimes referred to as the 'amount of turbulence induced fading'. The log normal model is valid for $\sigma_l^2 < 1.2$ [9]. Beyond this value, the effect of saturation, which is not accounted for by the log normal model, must be taken into account. Turbulence in-

duced irradiance fluctuation (scintillation) can enter saturation due to one or a combination of increased C_n (index of refraction structure parameter), link length and reduced wavelength [9], [19]. Experimental work carried out have however shown that the scintillation index does not only saturate, but it reaches a maximum value and then starts to decrease as the strength of turbulence increases [19]. In order to capture the turbulence effects across all regimes, here we consider the following models:

A. Gamma-Gamma Model

The gamma-gamma turbulence model proposed by Andrews *et al.* [18] is based on the modulation process where the fluctuation of light radiation traversing turbulent atmosphere is assume to consist of small scale (scattering) and large scale (refraction) effects. The former is contributed by the eddies cells smaller than the Fresnel zone or the coherence radius while the latter effect is due to the turbulence eddies greater than the first Fresnel zone or the scattering disk [18]. The small scale eddies are assumed to be modulated by the large scale eddies. Consequently, the received irradiance I is defined as the product of two statistically independent random processes I_x and I_y, that is

$$I = I_x I_y \qquad (1)$$

I_x and I_y arise from the large scale and small scale turbulent eddies respectively.

The gamma-gamma model for the probability density function (pdf) of received irradiance fluctuation which is based on the assumption that both the large and small scale effects are governed by the gamma distribution is therefore derived as [18], [22]

$$p(I) = \frac{2(\alpha\beta)^{(\alpha+\beta)/2}}{\Gamma(\alpha)\Gamma(\beta)} I^{(\frac{\alpha+\beta}{2})-1} \mathrm{K}_{\alpha-\beta}(2\sqrt{\alpha\beta I}) \quad I > 0 \quad (2)$$

where $\mathrm{K}_n(.)$ is the modified Bessel function of the 2nd kind of order n, and $\Gamma(.)$ represents the Gamma function. If the optical radiation is assumed to be a plane wave, the two parameters α and β that characterize the irradiance fluctuation pdf are related to the atmospheric conditions by [22]

$$\alpha = \left[\exp\left(\frac{0.49\sigma_l^2}{\left(1 + 1.11\sigma_l^{12/5}\right)^{7/6}} \right) - 1 \right]^{-1}$$

$$\beta = \left[\exp\left(\frac{0.51\sigma_l^2}{\left(1 + 0.69\sigma_l^{12/5}\right)^{5/6}} \right) - 1 \right]^{-1} \qquad (3)$$

where $\sigma_l^2 = 1.23 C_n^2 k^{7/6} L^{11/6}$ is the log irradiance variance, L is the link range, $k = 2\pi/\lambda$, and the refractive index structure parameter which is constant for an horizontal link is assumed the value $C_n^2 = 5.10^{-13} \mathrm{m}^{-2/3}$.

The pdf of irradiance fluctuation given by (2) is valid for all turbulence scenarios from weak to strong [18] and the values of α and β at any given regime can be obtained from (3). In this work, the values of the log intensity variance σ_l^2 corresponding to the weak, moderate and strong atmospheric turbulence regimes are given in Table I.
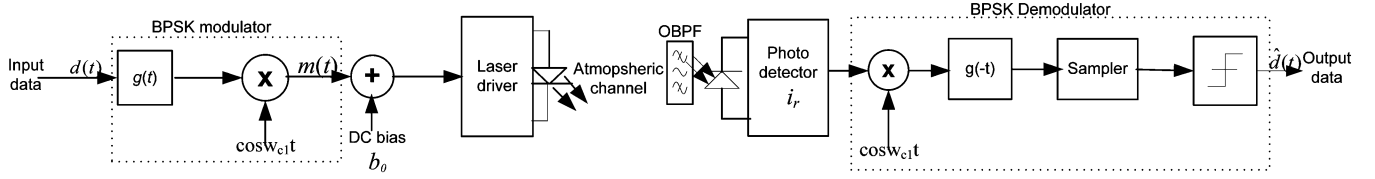
Fig. 1. Block diagram of BPSK subcarrier intensity modulated FSO link.

Parameter	Turbulence regime		
	weak	moderate	strong
σ_l^2	0.2	1.6	3.5
α	11.6	4.0	4.2
β	10.1	1.9	1.4

B. Negative Exponential Model

In the limit of strong irradiance fluctuations (i.e., in saturation regime and beyond) where the link length spans several kilometers, the number of independent scatterings becomes large [19]. The amplitude fluctuation of the field traversing the turbulent medium in this situation is generally believed and experimentally verified [7], [19], [20] to obey the Rayleigh distribution implying negative exponential statistics for the irradiance. That is

$$p(I) = \frac{1}{I_o} \exp(-I/I_o), \quad I_o > 0 \qquad (4)$$

where $\mathrm{E}[I] = I_o$ is the mean irradiance which is often normalized to unity. It should be noted that the gamma-gamma turbulence model also gives the negative exponential in the limit of strong turbulence [17], [18].

III. SUBCARRIER MODULATION

In optical SIM links, an RF subcarrier signal pre-modulated with the source data $d(t)$ is used to modulate the intensity of the optical carrier—a continuous wave laser diode. Fig. 1 illustrates the system model of a subcarrier intensity modulated FSO link. Prior to modulating the laser irradiance, $d(t)$ is modulated onto the RF subcarrier signal using BPSK in which bits '1' and '0' are represented by two different phases 180^0 apart. Since the subcarrier signal $m(t)$ is sinusoidal having both positive and negative values, a DC level b_0 is added to $m(t)$ before it is used to drive the laser diode. This is to ensure that the bias current is always equal to or greater than the threshold current.

Hence, the radiated optical signal is proportional to $m(t)$. At the receiver, the incoming optical radiation is passed through an optical band pass filter (OBPF) before being converted into an electrical signal by direct detection PIN photodetector. A standard RF coherent demodulator is employed to recover the source data $\hat{d}(t)$ as shown in Fig. 1, the OBPF is used to limit the

amount of background radiation noise detected by the photodetector. With intensity modulation and direct detection scheme the photocurrent is always proportional to $m(t)$; the instantaneous photocurrent $i_r(t)$ is thus given as:

$$i_r(t) = RI(1 + \xi m(t)) + n(t) \qquad (5)$$

where $I = 0.5I_{\mathrm{peak}}$, I_{peak} is the peak received irradiance, ξ is the modulation index, R is the photodetector responsivity, and $n(t) \sim N(0, \sigma^2)$ is the additive white Gaussian noise comprising of the thermal noise and the background radiation shot noise, i.e., $\sigma^2 = \sigma_{\mathrm{Thermal}}^2 + \sigma_{Bg}^2$. Considering a single symbol duration $m(t) = A(t)g(t)\cos(w_c t + \theta)$, where $A(t)$ is the subcarrier amplitude and $g(t)$ is the rectangular pulse shaping function. To keep the optical transmitter within its dynamic range and to avoid over-modulation induced clipping, the condition $|\xi m(t)| \leq 1$ must always be fulfilled.

IV. BIT ERROR RATE ANALYSIS

In the SIM hereby considered, each subcarrier signal is pre-modulated with the data using BPSK. The received signal (with the DC component filtered out) over a symbol duration, T is thus

$$i_r(t) = d_j RI\xi Ag(t)\cos(w_c t) + n(t) \qquad (6)$$

where $d_j \in \{1, -1\}$ is the signal level for the jth data symbol corresponding to the data symbols '1' and '0' and A is the fixed subcarrier amplitude. The threshold level is then fixed at the zero mark thereby eliminating the need for adaptive threshold, which poses implementation difficulty for the optimum performing OOK modulated FSO link in atmospheric turbulence [10], [14], [22]. Considering the additive white Gaussian noise from both the background radiation and the receiver electronics thermal noise [8], [14], the post detection electrical signal-to-ratio (SNR_e) ratio at the input of the BPSK demodulator is given by:

$$\mathrm{SNR}_e = \frac{(IR\xi)^2 P_m}{2B_{el}(qRI_{Bg} + 2kT_e/R_L)} \qquad (7)$$

where $P_m = (1/T)\int_T m^2(t)dt$ is the subcarrier signal power, B_{el} is the post detection electrical filter bandwidth required to pass $m(t)$ without distortion, q and k are the electronic charge and the Boltzmann's constant, respectively. I_{Bg} represents the background radiation irradiance while T_e and R_L are the temperature and the receiver circuit load resistance, respectively. Following the BPSK coherent detection, the baseband signal $i_d(t) = d_j RI\xi(A/2) + n_d(t)$, where $n_d(t) \sim N(0, \sigma^2/2)$. For

an equiprobable data symbols, the BER is given by the probability of $i_d(t) > 0$ when a data symbol '0' was transmitted. Hence, the following gives the unconditional BER:

$$P_e = \int_0^\infty \int_0^\infty \frac{1}{\sqrt{\pi}\sigma} \exp\left[-\frac{(i_d + 0.5RI\xi A)^2}{\sigma^2}\right] p(I) di_d dI$$

$$= \int_0^\infty Q(IRA\xi/\sqrt{2\sigma^2}) p(I) dI. \qquad (8)$$

It should be noted that the noise variance at the BPSK modulator input, $\sigma^2 = 2B_{el}(qRI_{Bg} + 2kT_e/R_L)$.

A. No Diversity

To evaluate the performance from weak to strong turbulence regime, (2) is substituted into (8) to obtain the BER expression given by (9). The values of the parameters α and β are as given in Table I. This BER expression has no closed form and it is therefore evaluated numerically

$$P_e = \int_0^\infty Q(RAI/\sqrt{2\sigma^2}) \frac{2(\alpha\beta)^{(\alpha+\beta)/2}}{\Gamma(\alpha)\Gamma(\beta)}$$

$$\times I^{(\frac{\alpha+\beta}{2})-1} K_{\alpha-\beta}(2\sqrt{\alpha\beta I}) dI. \qquad (9)$$

In the limit of strong turbulence that is in the saturation regime and beyond, the BER is obtained by substituting (4) into (8). Assuming $E[I] = I_o = 1$ and using the fact that for $x > 0$, $Q(x) = (1/\pi) \int_0^{\pi/2} \exp(-(x^2/2\sin^2\vartheta) d\vartheta)$, the BER is thus obtained as

$$P_e = \frac{1}{\pi} \int_0^{\pi/2} \int_0^\infty \exp\left(-\frac{(\xi RAI)^2}{4\sigma^2 \sin^2\vartheta} - I\right) dI d\vartheta. \qquad (10)$$

The multiple integration involved (10) can be conveniently circumvented by invoking equation (3.322.2) in [23]. This reduces the BER expression to

$$P_e = \frac{1}{\pi} \int_0^{\pi/2} \sqrt{\pi K(\vartheta)} \exp\left(K(\vartheta)\right) \text{erfc}\left(\sqrt{K(\vartheta)}\right) d\vartheta \qquad (11)$$

where $K(\vartheta) = (\sigma \sin\vartheta/\xi RA)^2$ and $\text{erfc}(x)$ is the complementary error function.

The resulting expression (11) has no closed form; and the following upper bound is obtained by maximizing the integrand by making $\vartheta = \pi/2$.

$$P_e \leq \sqrt{\pi K} \exp(K) Q(\sqrt{2K}) \qquad (12)$$

where $K = \sigma^2/(\xi RA)^2$.

From the BER expressions, the error performance of the system can be predicted for any given value of SNR. To illustrate this, the numerical simulations of BER expressions (9), (11) and the upper bound (12) are shown in Fig. 2(a) where the P_e is plotted against the normalized $\text{SNR} = (RE[I])^2/\sigma^2$ for all turbulence regimes. It should be said that the normalized
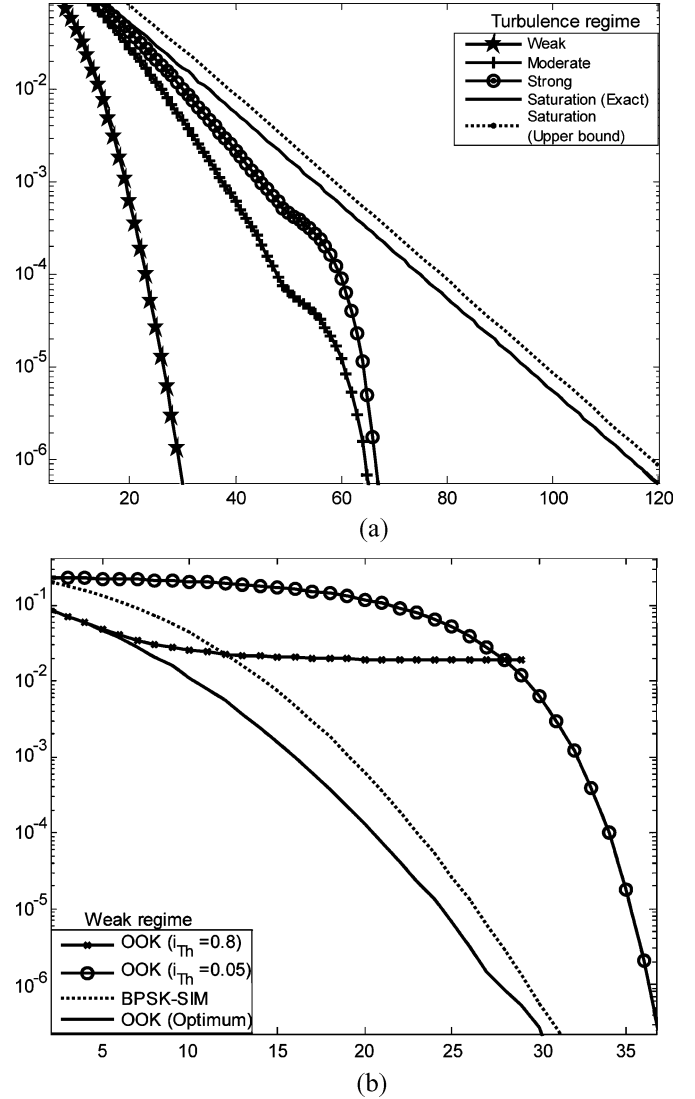

Fig. 2. (a) BER performance against the normalized electrical SNR with no diversity across all of turbulence regimes, $E[I] = R = A = 1$. (b) BER against the normalized electrical SNR in weak atmospheric turbulence using the SIM and OOK with fixed and adaptive threshold.

SNR is in the electrical domain and it is based on the average received irradiance, $E[I]$. For instance, to achieve a BER of 10^{-6} in a weak turbulence, the required SNR is ~ 29 dB and this rises to ~ 65 dB and ~ 67 dB, respectively for moderate and intermediate regimes. While in saturation regime, a staggering ~ 115 dB (the upper bound value is 4 dB higher) is required to achieve the same level of error performance (i.e., BER of 10^{-6}). Achieving a BER lower than 10^{-6} in the saturation regime requires a phenomenal increase in SNR as depicted by Fig. 2.

To compare the SIM with an OOK system, the average transmit irradiance is made equal to the SIM system. The received signal in an OOK system is therefore given by (13)

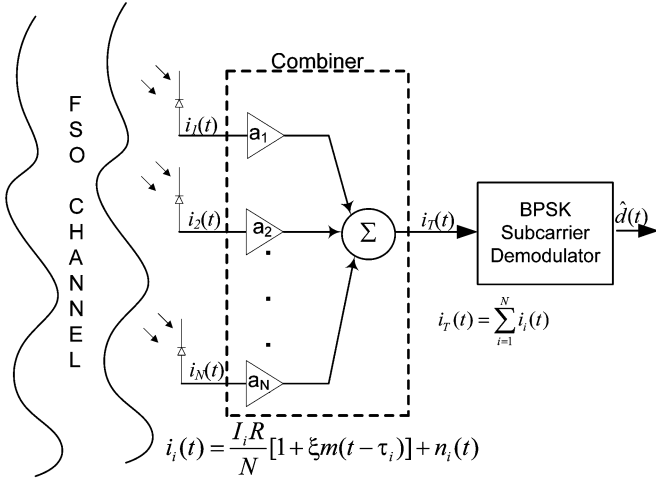$$i_r(t) = RI\left[1 + \sum_{j=-\infty}^\infty d_j g(t - jT)\right] + n_d(t). \qquad (13)$$

Fig. 3. Spatial diversity receiver block diagram.

Following the approach detailed in [14], the unconditional BER can be obtained as

$$P_{eOOK} = 0.5 \int_{i_{Th}}^{\infty} \frac{1}{\sqrt{\pi}\sigma} \exp\left(-i_r^2/\sigma^2\right) di_r$$

$$+ 0.5 \int_{0}^{\infty} \int_{0}^{i_{Th}} \frac{1}{\sqrt{\pi}\sigma} \exp\left[-(i_r - 2RI)^2/\sigma^2\right] p(I) di_r dI. \quad (14)$$

In Fig. 2(b), the BER performances of the OOK, system employing adaptive (optimum) and fixed threshold values of 0.05 and 0.8 are shown alongside that of BPSK-SIM in weak turbulence induced fading. Though, the optimum OOK is marginally superior at high SNR (requires 1.6 dB electrical SNR less than the BPSK-SIM at same BER of 10^{-6}); it does require an accurate knowledge of both the additive noise and fading levels. This is not practical/implementable as pointed out in [8]. With the threshold fixed at say 0.05, the OOK requires about 7 dB electrical SNR more than BPSK-SIM at a BER of 10^{-6}. Also, the BER performance of OOK with a fixed threshold level exhibits BER floor as shown in Fig. 2(b) for $i_{Th} = 0.8$ and in the previous work by [8] and the references there in. The SIM is therefore proposed over the fixed threshold OOK.

B. With Spatial Diversity

To further improve the error performance, the turbulence induced irradiance fluctuation is mitigated by employing multiple photodetectors that are sufficiently spaced to avoid any correlation in the received irradiance—see Fig. 3. That is, the spacing is assumed to be greater than the transverse correlation size ρ_o of the laser radiation. This assumption is realistic because the transverse correlation distance of the laser radiation in atmospheric turbulence is in the order of a few centimeters [9]. Also, to ensure fair comparison; each receiver aperture area of the N-photodetector array is made $(1/N)$th the receiver aperture size when a single photodetector is used.

The unconditional BER is thus given by

$$P_e = \int_{0}^{\infty} Q\left(\sqrt{\gamma_T(\vec{I})}\right) p(\vec{I}) d\vec{I} \quad (15)$$

where γ_T represents the post detection electrical SNR_e at the BPSK demodulator input and $p(\bar{I}) = \prod_{i=1}^{N} p(I_i)$ is the joint pdf of the uncorrelated irradiance. In determining γ_T, the equal gain combining (EGC) spatial diversity technique is considered. The EGC combiner sets $a_i = 1; i = 1, 2 \ldots N$, and requires the knowledge of the propagation delay, τ_i (phase shift) [24] on each diversity branch in order to obtain $i_T = (R/N) \sum_{i=1}^{N} [I_i + I_i d_j \xi A g(t) \cos(w_c t)]$, which is the coherent sum of the branch signals. This need for the knowledge of the phase shift/propagation delay on each diversity branch by the EGC combiner adds to the EGC receiver complexity but at the benefit of improved performance. At the combiner output, the signal power is $((R\xi A/(\sqrt{2}N)) \sum_{i=1}^{N} I_i)^2$ and the total noise variance, $\sigma_{EGC}^2 = N\sigma_{Thermal}^2 + \sigma_{Bg}^2$. Using an optical bandpass filter combined with narrow field of view detectors, the background noise can be reduced considerable. Hence, $\sigma_{Bg}^2 < N\sigma_{Thermal}^2$ and $\sigma_{EGC}^2 \geq N\sigma_{Thermal}^2$; the optimum post detection γ_T at the BPSK demodulator input is thus obtained as

$$\gamma_T = \frac{R^2 \xi^2 A^2}{2N^3 \sigma^2} \left(\sum_{i=1}^{N} I_i\right)^2. \quad (16)$$

The system performance with the spatial diversity in weak to strong turbulence regimes can thus be obtained from (2), (15) and (16) using numerical integration since the resulting expression has no closed form. However, in the limit of strong turbulence and considering the same EGC linear combining, the BER expression can be reduced to one involving single integration as follow. Let the random variable Z represent the sum of N independent negative exponential irradiance distribution i.e., $Z = \sum_{i=1}^{N} I_i$. The pdf of Z is quite straight forward by employing the characteristic function approach, thus

$$p(Z) = \frac{I_o^{-N} Z^{N-1} \exp(-Z/I_o)}{\Gamma(N)} \quad Z \geq 0. \quad (17)$$

The unconditional BER with receiver spatial diversity under negative exponential turbulence can now be obtained as

$$P_e = \frac{1}{\pi \Gamma(N)} \int_{0}^{\pi/2} \int_{0}^{\infty} Z^{N-1} \exp\left(-K_1(\vartheta)Z^2 - Z\right) dZ d\vartheta \quad (18)$$

where $K_1(\vartheta) = (R\xi A)^2/4N^3\sigma^2 \sin^2\vartheta$. Equation 18 has no closed form but the multiple integral involved is eliminated by invoking equation (3.462) reported in [23] to obtain the following expression for the BER:

$$P_e = \frac{1}{\pi} \int_{0}^{\pi/2} \frac{1}{\sqrt{(2K_1(\vartheta))^N}}$$

$$\times \exp\left(1/8K_1(\vartheta)\right) D_{-N}\left(1/\sqrt{2K_1(\vartheta)}\right) d\vartheta \quad (19)$$
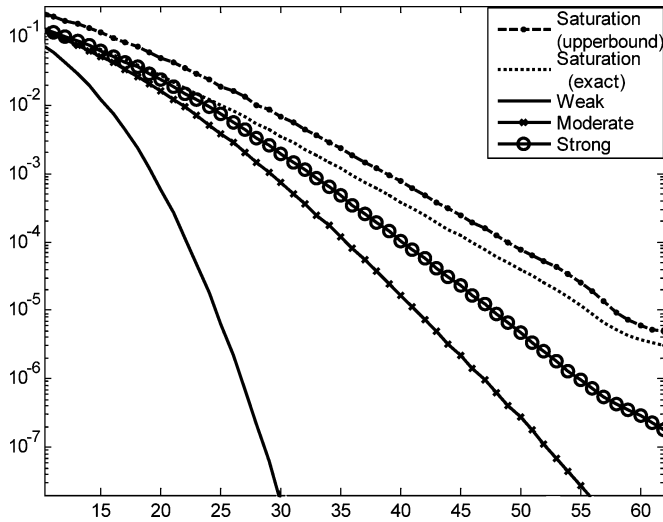
Fig. 4. BER performance against the normalized SNR using two photodetectors across Different turbulence regimes, $E[I] = \zeta = R = A = 1$.

TABLE II
DIVERSITY GAIN AT DIFFERENT TURBULENCE REGIMES (BER OF 10^{-6})

Number of photodetectors	Spatial diversity gain (dB)		
	weak	strong	saturation
2	2.6	11.6	46.7
3	3.0	21.2	63.6

To obtain an upper bound for the BER given by (20), the same approach of Section IV-A is used

$$P_e \leq \frac{1}{2\sqrt{(2K_1)^N}} \exp(1/8K_1) D_{-N}(1/\sqrt{2K_1}) \qquad (20)$$

where $K_1 = (R\xi A)^2/4N^3\sigma^2$ and D_ρ is the parabolic cylinder function [23].

The results obtained in this section are plotted in Fig. 4 for $N = 2$ (two photodetectors). When compared with Fig. 2(a), this graph reveals the reduction in the SNR brought about by the use of spatial diversity in mitigating the effect of turbulence induced irradiance fluctuation. As expected the impact of diversity is least in weak turbulence regime resulting in only 2.6 dB reductions in the SNR at BER of 10^{-6}. Whereas the for the strong turbulence regime, the gain in SNR is about 12 dB and $\sim$47 dB in the saturation regime. As would be expected, the diversity gain is highest in extreme fading conditions since adding more branches will greatly reduce the chance of a catastrophic fading from happening. A summary of the resulting diversity gain (i.e., reduction in the SNR) using two and three photodetectors at BER of 10^{-6} is presented in Table II.

V. CONCLUSION

The BER expression for SIM terrestrial FSO link has been presented in all turbulence regimes from weak to saturation. The gamma-gamma distribution is used to model atmospheric turbulence irradiance fluctuation in weak to strong turbulence

regimes while negative exponential distribution is adopted in the limit of strong turbulence. Spatial diversity has been considered to mitigate irradiance fluctuation and the corresponding BER and the upper bound presented. To obtain BER of 10^{-6} for instance, $\sim$29 dB of SNR is required in weak turbulence characterized by log intensity variance σ_l^2 of 0.2. The value of the required SNR increases as the turbulence level rises expectedly. With spatial diversity employing two photodetectors, up to 12 and 47 dB reduction in the the electrical SNR is predicted at a BER of 10^{-6} in strong turbulence ($\sigma_l^2 = 1.6$) and saturation regimes, respectively. The diversity gain is however achieved at the cost of increased receiver complexity and to attain the predicted diversity gains, the photodetectors must receive uncorrelated radiations.

REFERENCES

[1] H. Willebrand and B. S. Ghuman, *Free Space Optics: Enabling Optical Connectivity in Today's Network.* Indianapolis, IN: SAMS, 2002.

[2] D. Killinger, "Free space optics for laser communication through the air," *Opt. Photon. News*, vol. 13, no. 3, pp. 36–42, Oct. 2002.

[3] I. I. Kim, B. McArthur, and E. Korevaar, "Comparison of laser beam propagation at 785 nm and 1550 nm in fog and haze for optical wireless communications," in *Proc. SPIE Opt. Wireless Commun. III*, 2001, vol. 4214, pp. 26–37.

[4] K. Wakafuji and T. Ohtsuki, "Performance analysis of atmospheric optical subcarrier-multiplexing systems and atmospheric optical subcarrier-Modulated code-division multiplexing systems," *J. Lightw. Technol.*, vol. 23, no. 4, pp. 1676–1682, Apr. 2005.

[5] T. Kamalakis, T. Sphicopoulos, S. S. Muhammad, and E. Leitgeb, "Estimation of the power scintillation probability density function in free-space optical links by use of multicanonical Monte Carlo sampling," *Opt. Lett.*, vol. 31, pp. 3077–3079, Nov. 2006.

[6] X. Zhu and J. M. Kahn, "Performance bounds for coded free-space optical communications through atmospheric turbulence channels," *IEEE Trans. Commun.*, vol. 51, no. 8, pp. 1233–1239, Aug. 2003.

[7] A. Garcia-Zambrana, "Error rate performance for STBC in free-space optical communications through strong atmospheric turbulence," *IEEE Commun. Lett.*, vol. 11, no. 5, pp. 390–392, May 2007.

[8] J. Li, J. Q. Liu, and D. P. Taylor, "Optical communication using subcarrier PSK intensity modulation through atmospheric turbulence channels," *IEEE Trans. Commun.*, vol. 55, no. 8, pp. 1598–1606, Aug. 2007.

[9] G. R. Osche, *Optical Detection Theory for Laser Applications.* Hoboken, NJ: Wiley, 2002.

[10] W. Huang, J. Takayanagi, T. Sakanaka, and M. Nakagawa, "Atmospheric optical communication system using subcarrier PSK modulation," in *Proc. IEEE ICC*, May 1993, vol. 3, pp. 1597–1601.

[11] E. J. Lee and V. W. S. Chan, "Optical communications over the clear turbulent channel using diversity," *IEEE J. Sel. Areas Commun.*, vol. 22, no. 9, pp. 1896–1906, Nov. 2004.

[12] V. W. S. Chan, "Free-space optical communications," *J. Lightw. Technol.*, vol. 24, no. 12, pp. 4750–4762, Dec. 2006.

[13] M. Uysal, L. Jing, and Y. Meng, "Error rate performance analysis of coded free-space optical links over gamma-gamma atmospheric turbulence channels," *IEEE Trans. Wireless Commun.*, vol. 5, no. 6, pp. 1229–1233, Jun. 2006.

[14] X. Zhu and J. M. Kahn, "Free-space optical communication through atmospheric turbulence channels," *IEEE Trans. Commun.*, vol. 50, no. 8, pp. 1293–1300, Aug. 2002.

[15] G. Keiser, *Optical Fiber Communications*, 3rd ed. New York: McGraw-Hill, 2000.

[16] R. Ramaswami and K. Sivarajan, *Optical Networks: A Practical Perspective, Second Edition: A Practical Perspective*, 2nd ed. New York: Morgan Kaufmann, 2002.

[17] M. A. Al-Habash, L. C. Andrews, and R. L. Phillips, "Mathematical model for the irradiance probability density function of a laser beam propagating through turbulent media," *Opt. Eng.*, vol. 40, pp. 1554–1562, 2001.

[18] L. C. Andrews, R. L. Phillips, and C. Y. Hopen, *Laser Beam Scintillation With Applications.* Bellingham, WA: SPIE, 2001.

[19] S. Karp, R. M. Gagliardi, S. E. Moran, and L. B. Stotts, *Optical Channels: Fibers, Cluds, Water and the Atmosphere*. New York: Plenum Press, 1988.

[20] S. G. Wilson, M. Brandt-Pearce, Q. Cao, and J. H. Leveque, "Free-space optical MIMO transmission with Q-ary PPM," *IEEE Trans. Commun.*, vol. 53, no. 8, pp. 1402–1412, Aug. 2005.

[21] W. O. Popoola, Z. Ghassemlooy, and E. Leitgeb, "Free-space optical communication in atmospheric turbulence using DPSK subcarrier modulation," presented at the 9th ISCTA, Ambleside, Lake District, U.K., 2007.

[22] W. O. Popoola, Z. Ghassemlooy, and E. Leitgeb, "Free-space optical communication using subcarrier modulation in gamma-gamma atmospheric turbulence," in *Proc. 9th ICTON*, Rome, Italy, 2007, vol. 3, pp. 156–160.

[23] I. S. Gradshteyn and I. M. Ryzhik, *Table of Integrals, Series, and Products*, 5th ed. London, U.K.: Academic, 1994.

[24] M. K. Simon and M.-S. Alouini, *Digital Communication Over Fading Channels*, 2nd ed. New York: Wiley, 2004.

Wasiu O. Popoola (S'08) received the ND in electrical engineering from The Federal Polytechnic, Ilaro, Nigeria, and later received the B.Sc. degree (first class hons) in electronic and electrical engineering from Obafemi Awolowo University, Ile-Ife, Nigeria. He received the M.Sc. degree (with distinction) in optoelectronic and communication systems from Northumbria University, Newcastle upon Tyne, U.K., in 2006, where he is currently working toward the Ph.D. degree.

He worked briefly as a Teaching Assistant at Nnamdi Azikiwe University, Nigeria, between 2003 and 2004. His research interests include optical communication (fiber and wireless), digital communication and digital signal processing. He also works as Research/Teaching Assistant in the Northumbria Communication Research Laboratory. His research is partly sponsored by the British government under the ORSAS award and he also holds Northumbria University research studentship.

Mr. Popoola is student member of IET and an associate member of the Institute of Physics (IoP).

Zabih Ghassemlooy (S'98–M'94–SM'02) received the B.Sc. degree (hons) in electrical and electronics engineering from the Manchester Metropolitan University, Manchester, U.K., in 1981, and the M.Sc. and Ph.D. degrees in optical communications from the University of Manchester Institute of Science and Technology (UMIST), Manchester, U.K., in 1984 and 1987, respectively with Scholarships from the Engineering and Physical Science Research Council, U.K.

From 1986–1987 he worked as a Demonstrator at UMIST and from 1987 to 1988 he was a Postdoctoral Research Fellow at the City University, London, U.K. In 1988 he joined Sheffield Hallam University as a Lecturer, becoming a Reader in 1995 and a Professor in Optical Communications in 1997. He was the Group Leader for Communication Engineering and Digital Signal Processing Subject Division, and also head of Optical Communications Research Group until 2004. In 2004 he moved to the University of Northumbria, Newcastle upon Tyne, U.K., as an Associate Dean for Research in the School of Engineering and Technology. In 2005 he became Associate Dean for Research and Head of Northumbria Communications Research Laboratories in the School of Computing, Engineering and Information Sciences. He was a Visiting Professor at the Ankara University, Turkey, and Hong-Kong Polytechnic University, and is currently a Visiting Professor at the Technological University of Malaysia. His research interests are in the areas of photonic networks, modulation techniques, high-speed optical systems, optical wireless communications, as well as optical fiber sensors.

Prof. Ghassemlooy was a recipient of the Tan Chin Tuan Fellowship in Engineering from the Nanyang Technological University in Singapore to work on the photonic technology in 2001. In 2006, he was awarded one of the best Ph.D. research supervisors at Northumbria University. He is the Editor-in-Chief of *The Mediterranean Journals of Computers and Networks*, and *Electronics and Communications*. He serves on the Editorial Committees of *International Journal of Communication Systems*, and the EURASIP *Journal of Wireless Communications and Networking, Contemporary Engineering Sciences, Research Letter in Signal Processing*, and also has served on the Publication Committee of the IEEE TRANSACTIONS ON CONSUMER ELECTRONICS on the editorial board of the Inter and the Sensor Letters. He is the founder and the Chairman of the International Symposium on Communication Systems, Network and Digital Signal Processing, a committee member of The International Institute of Informatics and Systemics, and is a member of technical committee of a number of international conferences. He is a College Member of the Engineering, and Physical Science Research Council, U.K. (2003–2009), and has served on a number international Research and Advisory Committees. He has received a number of research grants from U.K. Research Councils, European Union, Industry and U.K. Government. He has supervised a large number of Ph.D. students and has published over 300 papers. He is a co-editor of an IET book: *Analogue Optical Fibre Communications* (IET, 1995) the proceedings of the CSNDSP '08, '06, CSDSP'98, and the First International Workshop on Materials for Optoelectronics 1995, U.K. He is the Co-Guest Editor of a number of special issues: the *IET Proceeding Circuit, Devices and Systems,* August 2006, the *Mediterranean Journal of Electronics and Communications* on "Free Space Optics-RF," July 2006, the *IET Proceeding Journal* 1994, and 2000, and *International Journal of Communications Systems* 2000. From 2004–2006 he was the IEEE U.K./IR Communications Chapter Secretary, and from 2006–2009 he was the Vice-Chairman, and is currently Chairman.